Yu *et al. Energy Mater* 2024;4:400045
DOI: 10.20517/energymater.2023.150

Energy Materials

Mini Review

Open Access

Check for updates

Influences of deposition conditions on atomic layer deposition films for enhanced performance in perovskite solar cells

Bohao Yu[1,4], Jiawen Zhang[1], Yuzhao Yang[1,2,*], Dingshan Yu[3,*], Yaohua Mai[4], Xudong Chen[1,2,*]

[1]School of Chemical Engineering and Light Industry, Guangdong University of Technology, Guangzhou 510006, Guangdong, China.
[2]Guangdong Provincial Laboratory of Chemistry and Fine Chemical Engineering Jieyang Center, Jieyang 515200, Guangdong, China.
[3]Key Laboratory for Polymeric Composite and Functional Materials of Ministry of Education Guangdong Engineering Technology Research Center for High-Performance Organic and Polymer Photoelectric Functional Films, School of Chemistry, Sun Yat-sen University, Guangzhou 510275, Guangdong, China.
[4]Institute of New Energy Technology, Jinan University, Guangzhou 510632, Guangdong, China.

***Correspondence to:** Prof. Yuzhao Yang, School of Chemical Engineering and Light Industry, Guangdong University of Technology, No. 100, Waihuan West Road, Higher Education Mega Center, Panyu District, Guangzhou 510006, Guangdong, China; Guangdong Provincial Laboratory of Chemistry and Fine Chemical Engineering Jieyang Center, Yuedong New Town University Road, Jieyang 515200, Guangdong, China. E-mail: yangyuzh@gdut.edu.cn; Prof. Dingshan Yu, Key Laboratory for Polymeric Composite and Functional Materials of Ministry of Education Guangdong Engineering Technology Research Center for High-Performance Organic and Polymer Photoelectric Functional Films, School of Chemistry, No. 132, Waihuan East Road, Higher Education Mega Center, Panyu District, Sun Yat-sen University, Guangzhou 510275, Guangdong, China. E-mail: yudings@mail.sysu.edu.cn; Prof. Xudong Chen, School of Chemical Engineering and Light Industry, Guangdong University of Technology, No. 100, Waihuan West Road, Higher Education Mega Center, Panyu District, Guangzhou, 510006, Guangdong, China; Guangdong Provincial Laboratory of Chemistry and Fine Chemical Engineering Jieyang Center, Yuedong New Town University Road, Jieyang 515200, Guangdong, China. E-mail: chenxd@gdut.edu.cn

How to cite this article: Yu B, Zhang J, Yang Y, Yu D, Mai Y, Chen X. Influences of deposition conditions on atomic layer deposition films for enhanced performance in perovskite solar cells. *Energy Mater* 2024;4:400045. https://dx.doi.org/10.20517/energymater.2023.150

Received: 31 Dec 2023 **First Decision:** 21 Mar 2024 **Revised:** 12 Apr 2024 **Accepted:** 30 Apr 2024 **Published:** 15 May 2024

Academic Editor: Meicheng Li **Copy Editor:** Fangling Lan **Production Editor:** Fangling Lan

Abstract

Atomic layer deposition (ALD) is a key technology for fabricating functional layers in perovskite solar cells, as it can deposit pinhole-free films with atomic-level thickness and tunable composition on high-aspect-ratio surfaces. Various deposition conditions have significant effects on the growth, physical, and chemical properties of ALD films, which, in turn, critically influences the performance of associated devices. Here, we review the reaction mechanisms underlying ALD and summarize how variables, such as precursors, deposition temperatures, and

substrates, impinge upon the quality of ALD films and the related devices. We emphasize the role of substrate in determining the nucleation and growth behavior of ALD films, which has been overlooked in previous reviews. Finally, we highlight the potential application of ALD in efficient perovskite solar cells in terms of carrier transport, encapsulated, and buffer layers, especially for tandem cells.

Keywords: Atomic layer deposition, substrate, perovskite solar cells, tandem solar cells

INTRODUCTION

In recent years, atomic layer deposition (ALD)[1] has aroused much attention in the semiconductor fields such as corrosion[2], catalysis[3] and solar cells[4-8]. As for solar cells, perovskite solar cells (PSCs) have been widely investigated owing to their advantages such as tunable bandgap[9], high absorption coefficient[10] and versatile fabrication methods[11]. For the fabrication of carrier transport, sputtering buffer, and encapsulated layers of PSCs, ALD[12] is a unique technology for growth conformal film growth based on self-limiting surface reactions, as compared with other methods such as spin-coating, thermal evaporation, and magnetron sputtering[13]. As shown in Table 1, compared to other film deposition techniques such as physical (PVD)[14] and chemical vapor deposition (CVD)[6,15], ALD provides the distinctive capability to form monolayer films. This facilitates precise control over film thickness and composition, ensuring exceptional uniformity and conformality at the angstrom level. As illustrated in Figure 1, an ideal ALD process consists of the following four steps: Step 1: The precursor of the first reactant A is pulsed into the reaction chamber and adsorbed on the substrate surface; Step 2: After the surface adsorption is saturated, the surplus precursor and by-products are purged out of the reaction chamber with inert gas; Step 3: The precursor of the second reactant B is pulsed into the reaction chamber and undergoes reaction with precursor A on the surface to grow the A_xB_y film; and Step 4: After the reaction is complete, the surplus precursor and by-products are purged out of the reaction chamber with inert gas. Based on the above steps, a conformal, pinhole-free film is cyclically deposited layer-by-layer.

The physical and chemical properties of ALD films are strongly influenced by three main factors: precursors, deposition temperatures, and substrates. Metal and oxygen sources are commonly used as precursors to fabricate metal oxide films in PSCs[16]. The reaction precursors should effectively react with the surface groups of the material[17-20]. Secondly, they must have sufficient chemical stability and cannot decompose due to physical factors (temperature, pressure, *etc*.) or corrode the underlying material. Deposition temperature is another key factor influencing the quality of ALD films and the performance of devices. Too high deposition temperatures may lead to decomposition of perovskite and deterioration of device performance[21]. As for substrates, the sufficient adsorption of the precursor molecules on the high-aspect-ratio surface is the prerequisite for achieving an ideal ALD film[12], which we also demonstrated in our previous research on the application of ALD for PSCs and tandem solar cells[22]. Therefore, the surface properties of the substrate significantly influence the film quality of ALD, which cannot be ignored.

Previous review articles have examined the benefits of ALD in the realm of PSCs. Brinkmann *et al*. have investigated functional layers prepared by ALD for PSCs[16]. Very recently, Zhang *et al*. have discussed ALD-prepared buffer and encapsulation layers for enhancing the stability of PSCs[23]. To fabricate high-quality ALD films in PSCs and their related tandem solar cells, a comprehensive review of the selection of reaction precursors, deposition temperatures, and substrates is necessary. In this mini review, we explore the ALD reaction mechanisms and the effects of different reaction conditions, such as precursors and temperatures, especially the deposition substrates, on the film properties. Additional studies on ALD substrates in the semiconductor field are also summarized, which may have potential impacts and applications on the PSCs.

Table 1. Comparison of PVD, CVD, and ALD

Film deposition techniques	Deposition principle	Deposition pattern	Uniformity	Conformality	Expansibility	Degree of vacuum	Film thickness
PVD	Physical vapor deposition	Nucleation growth	High number of pinholes and particles exist	Low and only for flat substrate	Medium	High requirement for vacuum degree and sensitive to the change of vacuum degree	Nanometer level
CVD	Gas-phase chemical reaction	Nucleation growth	Low number of pinholes and particles exist	Medium	Low	Medium	Nanometer level
ALD	Surface saturated reaction	Layer-by-layer growth	Low number of pinholes and no particles	High	High	Low	Angstrom level

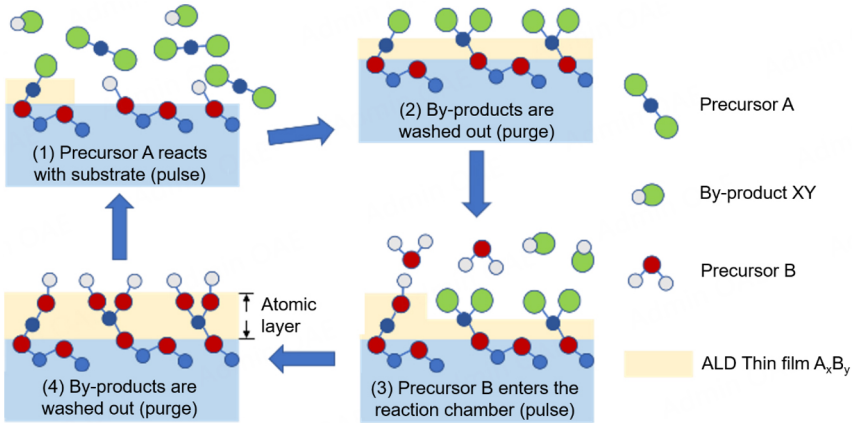

Figure 1. The reaction process of ALD.

EFFECT OF ALD REACTION CONDITIONS ON FILM PROPERTIES

Precursor

The underlying mechanism of precursor chemistry in ALD is predicated on the adsorption and subsequent reaction of precursor molecules onto the substrate surface[20]. So, ALD requires using highly reactive precursor molecules to interact selectively with the substrate surface. The chemical structure of the precursors also affects the surface chemistry and the growth rate of the film. As for PSCs, various metal oxides, such as ZnO, TiO_x, Al_2O_3, and SnO_x, are prepared by ALD as different functional layers, which respectively correspond to the metal precursors: diethyl zinc (DEZn)[24], titaniumtetrachloride ($TiCl_4$)[25], tetrakis(dimethylamido)titanium (TDMA-Ti)[26], Titanium isopropoxide (TTIP)[27], tris(dimethylamido)methylcyclopentadienyl titanium ($Ti(CpMe)(NMe_2)_3$)[28], trimethylaluminium (TMA)[29], and tetrakis(dimethylamido)tin (TDMA-Sn)[30,31]. The common oxygen precursors are H_2O, O plasma, O_3[32], and H_2O_2[33], which form the Metal-O bands. The selection of precursors may cause different effects on the reactant surface due to the different properties, such as strong Lewis acidity, and thus affect the performance of devices. The choice of inappropriate metal precursors will damage the substrate. Choudhury *et al.* reported that TMA precursors could break the interaction between PbI_3^- and $CH_3NH_3^+$, forming PbI_3-$Al(CH_3)_5$ and releasing CH_3NH_2 and CH_4[29]. These results revealed that they can damage the perovskite substrate. To further demonstrate, they observed an apparent mass loss due to the absence of $CH_3NH_3^+$ and the presence of only a PbI_2 peak in the X-ray diffraction (XRD) spectrum after 100 TMA pulses, which also confirms the decomposition of perovskite[29]. Hultqvist *et al.* investigated the compatibility of ALD directly deposited on the mixed halide perovskite. The Zn precursor DEZn was found

to exacerbate the degradation of the perovskite film, which converted into PbI_2 without forming ZnO. Different from the case of ZnO, the Sn precursor TDMASn did not degrade the perovskite, and conformal SnO_x films could be successfully formed[34], as shown in Figure 2A. Zardetto *et al.* compared ALD processes of Al_2O_3 and ZnO. They found that the DEZn precursor failed to react with the perovskite substrate to form ZnO films and instead caused the perovskite to decompose. A loss of 80% of the $MAPbI_3$ peak and a huge increase of the PbI_2 peak were observed in XRD analysis, which indicated the degradation of perovskite. In contrast, the evident growth of Al_2O_3 was observed, and the nitrogen peak intensity of perovskite did not decrease in the same situation [Figure 2B and C][35]. Kruszyńska *et al.* used DEZn/H_2O (AZO-1) and TMA/H_2O (AZO-2) to grow aluminum-doped zinc oxide (AZO) films[36]. They found that AZO-2 enhanced the thermal stability of the perovskite layer and facilitated charge transport at the interface. The better thermal stability of AZO-2 was explained by the weak acid-base reaction between ZnO and $MAPbI_3$. As for the charge transport, the increased carrier concentration improved the surface conductivity and electron mobility for AZO-2[36]. It can be seen from these results that the compatibility of metal precursors and substrates is very important.

As for oxygen precursors, it is worth mentioning that the exposure levels to a single pulse of H_2O are very low in the vacuum-based ALD process[35]. Thus, water is usually chosen as the oxygen source in the ALD of metal oxides. The influence of oxygen sources has also been investigated by several studies. Hu *et al.* reported a comparative study of SnO_x films and their devices prepared by ALD using H_2O, O_3 and plasma precursors as precursors[32]. It is found that the H_2O-based devices had the largest electron extraction barriers in the conduction band (CB) between PbI_2 and $MAPbI_3$, resulting in the poor ability of electron extraction. Additionally, the considerable gap states were found in H_2O-SnO_x, which were not found in the O_3- and plasma-based SnO_x layers. These gap states caused parasitic recombination and poor electron selectivity at the interface, resulting in low efficiency and large hysteretic for the devices based on H_2O-SnO_x[32]. Similarly, Zardetto *et al.* studied the impact of direct exposure of $MAPbI_3$ to H_2O and O_2 plasma. It is found that the decomposition effect was more evident when $MAPbI_3$ was directly exposed to the O_2 plasma [Figure 3A][35]. Behrendt *et al.* compared the characteristics of SnO_x films grown with O_3 and H_2O as oxygen source precursors[37], respectively, as shown in Table 2. Compared to H_2O-based layers, O_3-based layers had a trend of lower water vapor transmission rates (WVTR) with increasing deposition temperatures, which was related to the rising layer density. They had higher values for bandgap energy (E_g), which can be explained by particle size effects. Furthermore, the ALD SnO_x film prepared by O_3 source exhibited better transmittance in the visible region, while H_2O-based layers had poor transmittance due to subgap absorption[37], as shown in Figure 3B and C. Wang *et al.* compared ALD Al_2O_3 films prepared by low temperature using H_2O, O_2 plasma and O_3 as oxygen sources[38]. They proved that using O_2 plasma or O_3 as an oxygen precursor could make the film denser and grow at a higher rate under low temperature conditions [Figure 3D]. Compared with H_2O- and O_2 plasma-based films, the O_3-based film had the minimum root mean square (RMS) value, exhibiting a smooth surface. Fourier transform infrared (FTIR) spectroscopy analysis unveiled a significant presence of OCO, C-O, and C-H bonds in the H_2O-based film, whereas the lowest concentration of these carbon species was observed in the O_3-based film. The notable abundance of carbon species in the H_2O-based film may impede the self-limiting ALD reaction, consequently resulting in the formation of a film of inferior quality[38]. Compared with the H_2O precursor, Lee *et al.* discovered that the ALD-SnO_x layer fabricated using H_2O_2 exhibited enhanced electron extraction ability, attributed to a decrease in oxygen vacancies, which is associated with the highly oxidizing properties of H_2O_2[39]. The surface roughness reduced from 36.43 nm for H_2O-based films to 32.02 nm for H_2O_2-based ones. The reduced roughness of H_2O_2-based films exhibited better contact with the perovskite, leading to the enhanced open circuit voltage (V_{OC}) and fill factor (FF)[39].

Table 2. Properties of ALD SnO_x films using O_3 or H_2O as oxidants. Reprinted with permission from ref.[37]. Copyright 2015 Wiley

ALD-film	T_D [°C]	WVTR average [g (m² day)$^{-1}$]	Density ρ [g cm^{-3}]	σ [S cm^{-1}]	n [cm^{-3}]	μ [cm² Vs^{-1}]	Carbon content [%]	Nitrogen content [%]	[O]/[Sn]	E_g [eV]	T_{av} [%]
SnO_x (O_3)	100	2.2×10^{-4}	3.8	3×10^{-5}	-	-	12.8	6.7	2.6	4.23	89
	150	8.8×10^{-6}	4.8	2	2×10^{18}	5	7.3	5.4	2.3	3.88	84
	200	3.6×10^{-6}	7.0	3×10^{2}	2×10^{20}	10	1.8	1.4	2.1	3.67	80
SnO_x (H_2O)	100	7×10^{-5}	5.4	6×10^{-4}	1×10^{15}	4	3.6	2.1	2.2	3.80	78
	150	3×10^{-5}	5.3	3×10^{-3}	1×10^{16}	2	3.6	1.4	2.0	3.19	67
	200	3.1×10^{-6}	5.7	6×10^{-5}	-	-	1.9	0.3	1.8	3.21	69

The deposition temperature T_D, the water vapor transmittance WVTR, density ρ, conductivity σ, carrier density n, carrier mobility μ, [O]/[Sn] of 200 nm SnO_x and the data in % are expressed. The element content, band gap energy E_g, and transmittance T_{av} of 200 nm SnO_x are measured by RBS, which indicates that the meaningful data cannot be obtained with too low content.

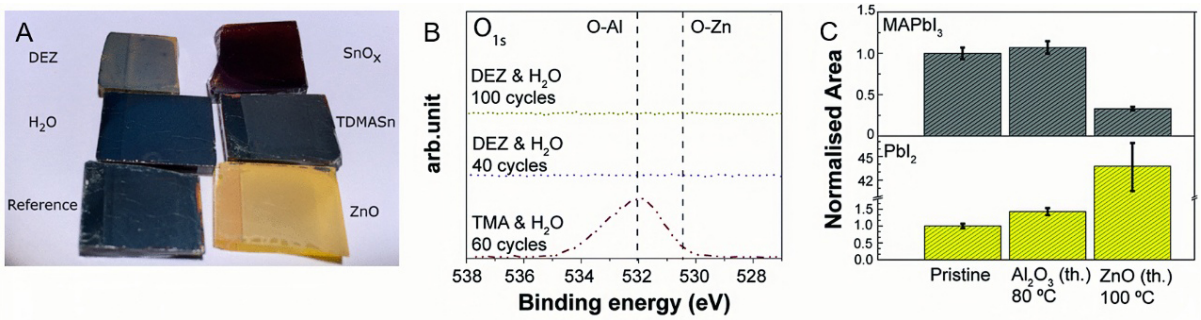

Figure 2. (A) Image showing perovskite films subjected to partial ALD treatments employing H_2O, DEZn, or TDMASn or subjected to complete ALD processes for either ZnO or SnO_x. Reprinted with permission from ref.[34]. Copyright 2017 American Chemical Society. (B) XPS pattern of O 1s spectra for three distinct perovskite samples: pristine, post thermal ALD Al_2O_3, and ZnO treatments. (C) Normalized areas of the $MAPbI_3$ {110} peak and PbI_2 {001} peak. Reprinted with permission from ref.[35]. Copyright 2017 Royal Society of Chemistry.

In summary, it is necessary to fully understand the compatibility between ALD precursors and the reactant substrate to keep a substrate from decomposition or degradation.

Deposition temperature

The deposition temperature is a critical factor in the growth of ALD films, significantly affecting the reaction kinetics and surface chemistry of the precursor molecules[20]. Notably, the growth rate of ALD films, quantified by the growth per cycle (GPC), is significantly influenced by temperature. It remains consistent within a specific range of deposition temperatures, ensuring adequate thermal energy for the chemical reactions involved in the ALD process. Beyond this range, it increases due to the disruption in the self-limitation caused by the thermal degradation of the metal precursor[40]. However, a contrary phenomenon is occasionally observed, where the growth rate decreases with the increasing growth temperature, possibly owing to insufficient precursor reaction or the condensation of the precursors[41]. Therefore, optimal temperatures are necessary to promote the chemisorption reactions and achieve desirable growth rates. As per previous reports, ALD can occur in different temperature ranges in a limited amount of time. In typical thermal ALD processes for metal oxides, temperatures ranging from 100 to 400 °C are commonly used[42]. Spatial ALD processes and plasma-assisted methods could facilitate processing temperatures below 100 °C[43-46]. Zardetto *et al.* explored the influence of deposition temperature on the perovskite layer. Samples were kept for 4 h at 30, 80 and 100 °C during the ALD process[35]. Compared to 30 and 80 °C, the XRD peak of $MAPbI_3$ decreased by almost 40%, and that of PbI_2 increased

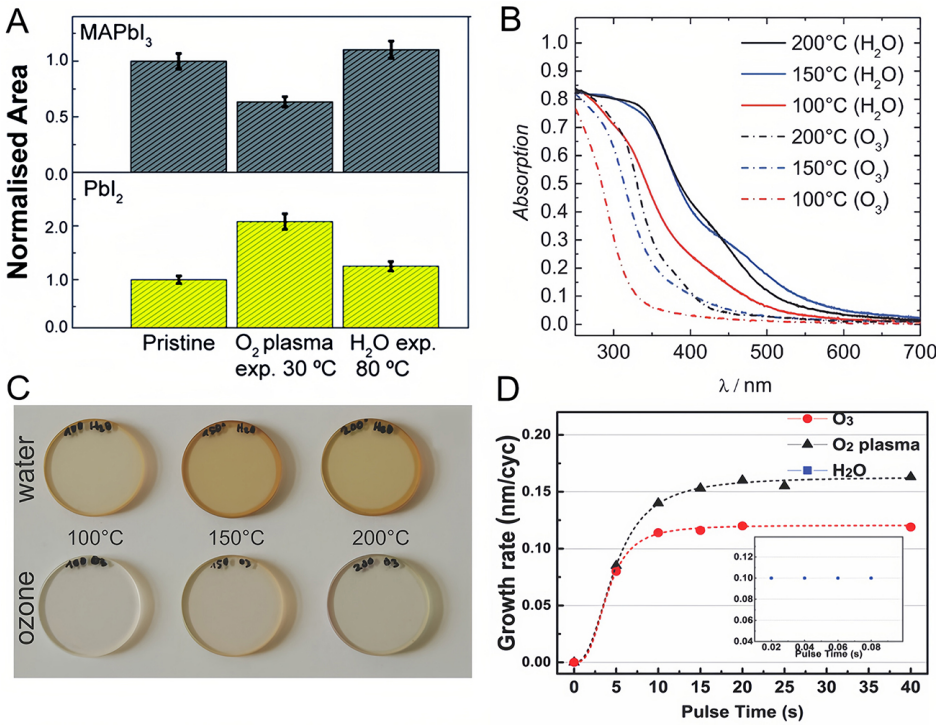

Figure 3. (A) Normalized areas of the $MAPbI_3$ {110} peak and PbI_2 {001} peak. Reprinted with permission from ref.[35]. Copyright 2017 Royal Society of Chemistry. (B) The optical absorption spectra of SnO_x layers synthesized at various temperatures using either O_3 or H_2O as oxygen source. (C) Images depicting SnO_x layers fabricated at different temperatures utilizing either O_3 or H_2O as oxygen source on quartz substrates. Reprinted with permission from ref.[37]. Copyright 2015 Wiley. (D) The growth per cycle plotted against the pulse time of oxidants, as determined from ellipsometry measurements. Reprinted with permission from ref.[38]. Copyright 2018 Wiley.

dramatically at 100 °C. The organic methylammonium component degraded into HI and CH_3NH_2 by-products due to the thermal stress, and they further sublimated and formed PbI_2. After only 1 h at 100 °C, no perovskite degradation was detected, indicating that the ALD processing time should be shortened when using a higher reaction temperature[35]. Lindahl *et al.* studied the structure and optical properties of zinc tin oxide (ZTO) films with growth temperatures between 90 and 180 °C. It is found that the growth temperature had minimal impact on the composition of the films. However, it significantly influenced the growth rate, density, and E_g of ZTO films[47]. As deposition temperatures rose, the density of ZTO films increased, while the E_g decreased, which was associated with the microstructural alterations of the ZTO films. Transmission electron microscopy (TEM) measurements showed that ZTO films contained small ZnO or ZnO (Sn) crystallites, and the size of these crystallites increased with rising Zn content and deposition temperature. They caused the quantum confinement effects to reduce the E_g due to the increased size[47]. Chistiakova *et al.* investigated the effect of temperature for two kinds of ALD processes: non-optimized (2 s, 150 W oxygen plasma treatment step) and optimized (6 s, 300 W oxygen plasma treatment step with an additional flow of 10 sccm of Ar)[48]. They found that the resistivity of ALD SnO_x layers decreased by 4-5 orders with increasing deposition temperature from 120 to 200 °C, and a slight decrease of resistivity also occurred for the non-optimized ALD process. The carbon and nitrogen contaminations on the SnO_x layer decreased with increasing temperature, resulting in the augmentation of the refractive index and the decline of the optical E_g due to the Burstein-Moss shift[48]. Köhnen *et al.* analyzed the relationship between optical properties and deposition temperatures in the deposition of SnO_x layers. The film exhibited higher ultraviolet (UV) absorption and refractive index at higher temperatures[49]. In addition, it is found that the deposition temperature had no effect on the short circuit current density (J_{SC}) and V_{OC} of PSCs,

while the FF reduced with the increasing deposition temperature from 80 to 120 °C[49]. In contrast, Hultqvist *et al.* found that the PSCs with SnO_x deposited at 60 °C exhibited lower V_{OC} and FF than those with SnO_x deposited at 90 °C owing to a double diode-like behavior[50].

In summary, the deposition temperature significantly influences the optical and electrical properties of the films. For example, the atoms of amorphous materials form electronic states at the edge of the energy band, which replace the electronic states at the tail of the energy band, leading to higher optical absorption and lower optical band gap[48,51].

THE REACTION SUBSTRATE OF ALD

The substrate type is integral to the deposition process, as it dictates the adsorption and subsequent reactions of precursor molecules[20]. The nature of the substrate can influence the nucleation and growth of the film and its properties, such as composition, crystallinity, and morphology. Variations in the surface structure and chemical makeup of substrates can lead to differential adsorption and reaction behaviors of the precursors, which, in turn, affect the growth rate and the ultimate properties of the film. The ALD procedure relies on self-terminating surface reactions, which are closely linked to the surface functionalities on the deposition substrates. ALD substrates can be classified into two major categories[22,52]: (1) unreactive substrates lacking nucleation sites for deposition; and (2) reactive substrates with abundant reactive sites. Puurunen *et al.* proposed that the ALD process transitioned into island growth when the substrate was unresponsive to the ALD reactant, a phenomenon also known as substrate-inhibited growth[52]. Compared with island growth, layer-by-layer growth is necessary to shape an extremely pinhole-free, conformal, and smooth surface that improves PSC performances[22,52]. The deposition mode of ALD is nonstatic. For instance, Stranski-Krastanov growth illustrates a scenario where ALD initially proceeds with layer-by-layer growth but transitions to island growth due to stress effects within the film[53,54]. According to the GPC, the growth mode can be further classified into three categories[18,52]: (1) Substrate-inhibited growth, where the GPC is primitively low (island growth) and then reaches a linear growth mode; (2) Linear growth, where the GPC is constant throughout the process of ALD; and (3) Substrate-enhanced growth, wherein the GPC exhibits elevated levels initially before transitioning into linear growth. The last two cases correspond to layer-by-layer growth mode[18].

Brinkmann *et al.* used a bistratal AZO/SnO_x electron transportation layer (ETL) to create excellent resilience against moisture and heat in PSCs. They discovered that the stability of the AZO/SnO_x devices was superior to that of the devices with SnO_x deposited directly on the surface of [6,6′]-phenyl-C61-butyric acid methyl ester (PCBM), which was attributed to the nonideal ALD growth of SnO_x directly on the surface of the unreactive PCBM layer[55]. Furthermore, Yu *et al.* discovered that ZnO could not nucleate on the PCBM surface. Subsequently, they utilized TMA, a potent Lewis acid, to react with the C=O groups present in PCBM. The Al_2O_3 could provide nucleation sites for the growth of ZnO[56]. Gong *et al.* used 2-mercaptoethanol (2-mcpEtOH) to modify the perovskite surface, allowing the S in the thiol group to bond with Pb^{2+} of perovskite. The modified layer provided the reactant sites -OH and thiol protons (SH) for ALD. Upon exposure to water, the surface exhibited stronger chemical resistance than a bare, unmodified perovskite film[57]. Wang *et al.* improved the PCBM surface by adding 3-aminopropyl triethoxysilane (APTS) molecules, which provided nucleation sites to form dense SnO_x films, improving the stability of inverted flexible PSCs[58]. As illustrated in Figure 4 of our previous study, Yu *et al.* reported that the nucleation of ALD SnO_x films was delayed on the unreactive substrate PCBM[22]. They activated the unreactive layer by introducing AZO with -OH groups. Through a combination of XPS and FTIR analysis, it was demonstrated that the modified PCBM layer provided adequate reactive sites for layer-by-layer growth, forming impermeable SnO_x films. Additionally, a significant increase in roughness was observed in

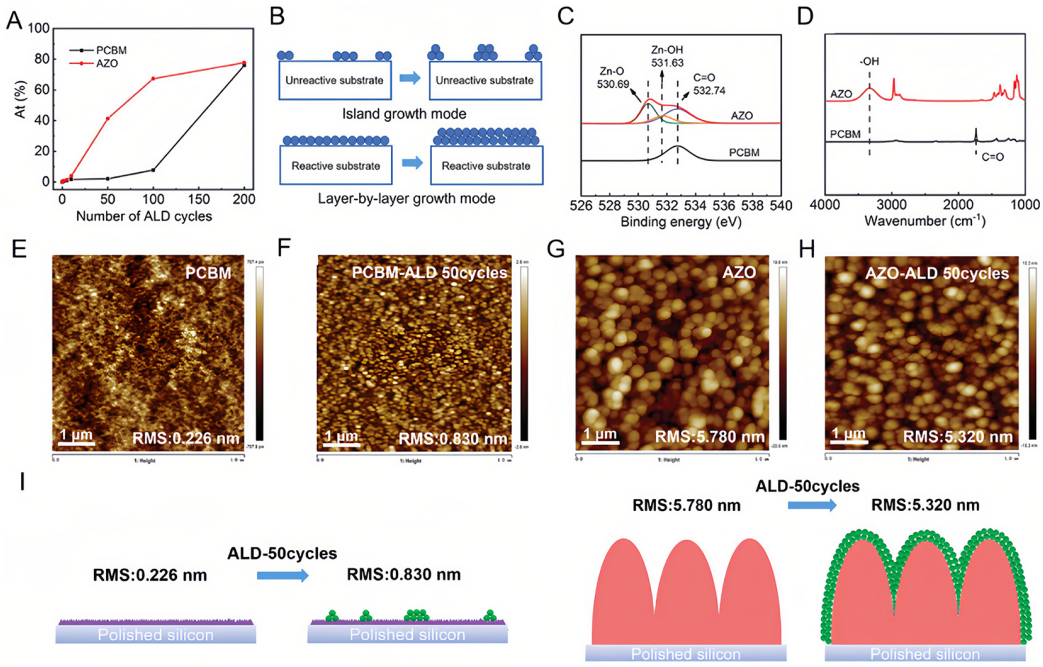

Figure 4. (A) Sn content (expressed as atomic percentage, At%) in relation to the number of SnO_x cycles. (B) A diagram of different deposition modes. (C) XPS spectra. (D) FTIR spectra. (E-H) AFM images. (I) Diagram of two deposition modes on PCBM and AZO substrates. Reprinted with permission from ref.[22]. Copyright 2023 Wiley.

the PCBM sample by AFM, indicating non-continuous island growth on the PCBM substrate, contrasting with the layer-by-layer growth on the AZO substrate. This discrepancy in growth behaviors was attributed to the island and layer-by-layer growth modes on the unreactive and reactive substrates, respectively[22]. Similarly, Liu *et al.* observed the island growth of ALD SnO_x on the unreactive substrate C_{60}, which caused the problem of excessive dark current of the device. To address this issue, WO_3 was added to the surface of C_{60}, and dense ALD films grown layer-by-layer were obtained[59].

Polyethyleneimine ethoxylated (PEIE) is an ideal material for ALD, which has a rich density of hydroxyl groups. ALD precursors can penetrate into polymer or small-molecule substrates, leading to sub-surface formation[60]. Instead of a chemically inert C_{60} surface, Palmstrom *et al.* used PEIE as a nucleation layer for recombination layers prepared by ALD in all-perovskite tandem cells[60]. Furthermore, metal oxides, including TiO_2, Al_2O_3, and SnO_x, were respectively deposited on C_{60} and PEIE substrates. The former ALD layers degraded significantly in solvents [water and dimethylformamide (DMF)], whereas the latter ALD films remained stable in solvents [Figure 5A]. The solvents-resistance property was enhanced by the more impermeable ALD film grown on the PEIE layer, which provided both hydroxyl and amine functional groups. These groups were suitable for nucleating and reacting with the precursors[60]. Besides, Li *et al.* introduced PEIE to facilitate the nucleation and crystal growth of perovskite films and provide surface reactive sites for ALD ZnO[61]. Raiford *et al.* also utilized PEIE to functionalize the surface of C_{60} for the subsequent deposition of ALD SnO_x and VO_x films, which served as barrier layers to improve the stability of PSCs[62]. It is seen that the nucleation of ALD SnO_x formed a more continuous and denser barrier layer after using PEIE, which exhibited excellent water vapor barrier performance and protected the perovskite film from degradation under high temperature (200 °C) and humidity conditions, as shown in Figure 5B. The unpackaged device with a Ag electrode still maintained 94% of the initial efficiency after 670 h of thermal aging at 85 °C, whereas the efficiency of similar devices without PEIE dropped to 0 at 670 h. In addition,

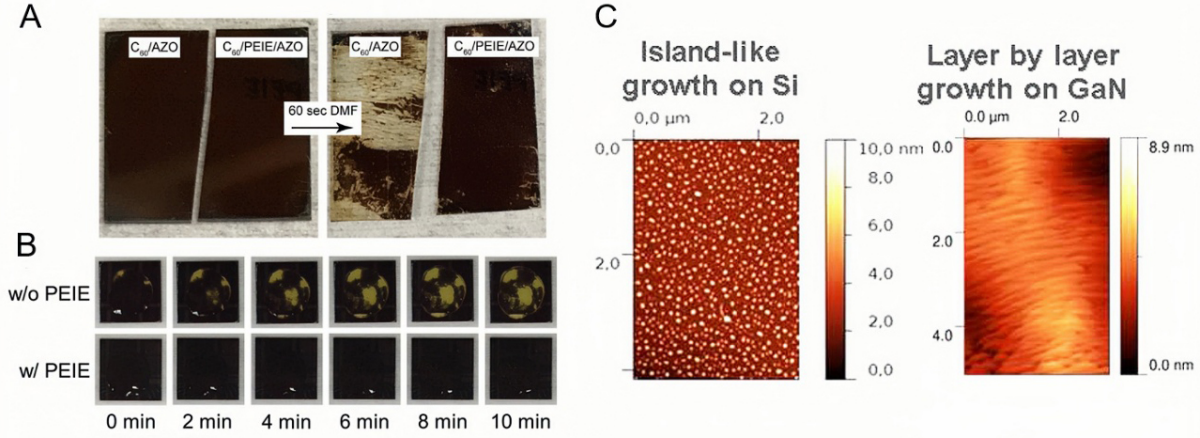

Figure 5. (A) Images of perovskite samples: before and after exposure to DMF for 60 s. Reprinted with permission from ref.[60]. Copyright 2019 Elsevier. (B) Time-lapse images of water-resistance test. Reprinted with permission from ref.[62]. Copyright 2019 Wiley. (C) AFM images of ALD ZnO films indicated the island-like growth on Si substrate and the layer-by-layer growth on GaN. Reprinted with permission from ref.[64]. Copyright 2012 American Chemical Society.

PEIE-based devices also showed better light stability[62]. Indeed, the substrate plays a significant role in determining the growth behavior of ALD films. Therefore, the substrate modification engineering is crucial for improving the quality of ALD films and the performance of PSCs. Table 3 summarizes the properties of ALD films prepared on different substrates and the stability performance of the corresponding PSCs. The modification of the substrate can form denser and smoother ALD thin films, which greatly improves the stability of the PSCs.

In addition to the perovskite field, the research on the ALD substrate is also carried out in other semiconductor fields, which have significant support for improving the performance of PSCs. Labbe *et al.* used TEM and spectroscopic ellipsometry (SE) to investigate the nucleation behavior of ALD FeO_x[53]. During the ALD process, both substrate-enhanced and substrate-inhibited growth modes were observed. They found that layer-by-layer growth did not always occur in the linear growth regime after island coalescence[53]. Moreover, several studies have indicated that the island growth mode is unfavorable for achieving high-quality ALD films. Yun *et al.* noted that during island growth, the nucleation stage of the ALD process exhibited nonideal behavior, impeding layer-by-layer growth and resulting in delayed nucleation[63]. This behavior was attributed to a deficiency in reaction sites, necessitating additional incubation cycles for nucleus formation. They further explored the nucleation and growth behavior of AlN film on Si and TiN substrates by thermal ALD. The nucleation of AlN films was delayed on the Si substrates, while they grew without any nucleation delay on TiN substrates. The substrate-inhibited growth on Si surfaces was attributed to the scarcity of reactive sites, and ammonia (NH_3) pretreatment on Si surfaces was applied to grow uniform AlN films[63]. Baji *et al.* observed that the island growth occurred on the unreactive substrate Si, while it grew layer-by-layer on the reactive substrate GaN during the ALD deposition of ZnO. The latter had a smoother film than the former[64], as shown in Figure 5C. Uğur *et al.* also reported that island growth of Al_2O_3 occurred when the reactant materials were deposited on unreactive substrates. They observed through TEM that ALD Al_2O_3 could not completely cover the hexagonal boron nitride (hBN) substrate because of an unreactive substrate[65]. Hagen *et al.* found that the ALD Cu processes varied significantly depending on the substrate materials employed. On Si and TaN surfaces, isolated island formation was observed[66]. Polymers are special substrate materials for ALD processes as well. Wilson showed that Al_2O_3 films deposited by ALD on various polymer substrates, including polystyrene (PS), polypropylene (PP), poly(methyl methacrylate) (PMMA), polyethylene (PE), and poly(vinyl chloride)

Table 3. The properties of ALD films prepared on different substrates and the stability of the corresponding PSCs

ALD thin film	Substrate	Quality of ALD thin film	Storage condition	Stability of devices	Ref.
SnO_x	PCBM	Roughness increased from 0.226 to 0.830 nm after 50 cycles of SnO_x deposition	Ambient air (at 25 °C, 30%RH) for 75 h; N_2 atmosphere (at 25 °C) for 670 h; Heated at 85 °C in N_2 atmosphere for 700 h; Operated at ambient under 1 sun illumination for 32 h	Normalized PCE decreased to 0.77; Normalized PCE decreased to 0.73; Normalized PCE decreased to 0.81; Normalized PCE decreased to 0.80	[22]
	AZO	Roughness decreased from 5.780 to 5.320 nm after 50 cycles of SnO_x deposition	Ambient air (at 25 °C, 30%RH) for 2,300 h; N_2 atmosphere (at 25 °C) for 5,100 h; Heated at 85 °C in N_2 atmosphere for 1,580 h; Operated at ambient under 1 sun illumination for 1,000 h	Normalized PCE decreased to 0.84; Normalized PCE decreased to 0.99; Normalized PCE decreased to 0.81; Normalized PCE decreased to 0.84	
SnO_x	PCBM	Nonideal growth	Ambient air (at 22 °C, 60%RH) for 150 h	V_{OC} and FF decreased to 0	[55]
	AZO	Impermeable	Ambient air (at 22 °C, 60%RH) for 150 h	V_{OC} increased from 0.84 to 0.95, and FF decreased from 60% to 50%	
SnO_x	PCBM	Roughness of 8.32 nm; R_S of 64 Ω	Ambient air (at 25 °C, 85%RH) for 600 h	Normalized PCE decreased to 0.77	[58]
	APTS modified PCBM	Roughness of 4.29 nm; R_S of 46 Ω	Ambient air (at 25 °C, 85%RH) for 600 h	Normalized PCE decreased to 0.9	
SnO_x	C_{60}	Large SnO_x gains and lower atomic concentrations of Sn and C	Operated in ambient air (at 60 °C, 30%RH) under 0.77 sun illumination at 60 °C for 250 h; Heated at 85 °C in N_2 atmosphere for 700 h	Normalized Avg. P_{MAX} decreased to 0.585, Normalized Avg. V_{OC} decreased to 0.231; Normalized PCE decreased to 0	[62]
	PEIE	Small SnO_x gains and higher atomic concentrations of Sn and C	Operated in ambient air (at 60 °C, 30%RH) under 0.77 sun illumination at 60 °C for 250 h; Heated at 85 °C in N_2 atmosphere for 670 h	Normalized Avg. P_{MAX} decreased to 0.815, Normalized Avg. V_{OC} decreased to 0.585; Normalized PCE decreased to 0.94	

Relative humidity RH, open circuit voltage V_{OC}, fill factor FF, series resistance R_S, power conversion efficiency PCE, average maximum power Avg. P_{MAX}, average open circuit voltage Avg.

(PVC). TMA first diffused into the polymer and then reacts with H_2O on the substrate surface to form Al_2O_3, leaving some TMA unreacted[67]. A similar phenomenon was found by Jur *et al.*[68]. Demelius *et al.* investigated the PE-ALD growth of ZnO on polyethylene glycol dimethacrylate (pEGDMA) and poly 2-hydroxyethyl methacrylate (pHEMA)[69]. They discovered more intense precursor diffusion in pEGDMA with fewer reactive sites. The growth process of ZnO consisted of plasma etching of the polymer substrate and ALD growth of ZnO. Besides, they found that ZnO films were formed after 3-5 cycles on pHEMA using *in-situ* SE and X-ray reflectivity (XRR), whereas a significant nucleation delay after 12-16 cycles was detected on pEGDMA. By comparing the growth modes[52], island growth, as the dominant growth mode on pEGDMA, was found, while nucleation on pHEMA was more similar to layer-by-layer growth. These results revealed that the density of reactant sites affected the nucleation behavior for ALD substrates[69]. Weiß *et al.* compared the GPC of ALD CuO films on Si, Al_2O_3, and TiO_2 substrates at room temperature. The Si substrate had the highest GPC, but this phenomenon was not further explained[70]. Zhou *et al.* proposed a two-step interface engineering process (chemical mechanical polishing and RCA SC-2 treatment) to optimize the deposition process of ALD AlO_x and avoid substrate-inhibited growth, thereby improving the ALD surface quality and wettability[71]. In addition, introducing seed layers, such as Al_2O_3[56,72,73] and black phosphorus[74], was often an effective way to activate unreactive substrates.

THE APPLICATIONS OF ALD FOR ENHANCED PERFORMANCE IN PSCS

As shown in Figure 6, ALD enables the precise and conformal deposition of materials in various types of PSCs, including scalable, flexible and tandem solar cells. The efficiency of the PSCs always suffers from charge recombination loss because of defects in bulk or at interfaces[75-77]. Therefore, surface passivation strategy and interface engineering are needed to reduce the nonradiative recombination and enhance charge carrier transportation and collection. In some aspects, the ALD layer presents a viable approach to address these challenges, improving performance of various types of PSCs.

ALD enables preparation at a low temperature, making it particularly suitable for PSC fabrication. Based on the discussion of the precursor and deposition temperature section, it is known that organic-inorganic hybrid perovskites are nature-sensitive with precursors and deposition temperatures. Zhao et al. also found that perovskite degraded when the deposition temperature was higher than 125 °C and chose 75 °C as the best deposition temperature to grow Al_2O_3[21]. Then, ALD Al_2O_3 deposited at 75 °C was used to sufficiently passivate defect states at the surface of perovskite. After interface passivation via ten cycles of the ALD Al_2O_3 layer, the efficiency of the device enhanced from 18.8% to 20.0%. The ALD Al_2O_3-based devices can maintain more than 95% of their initial efficiency after being stored in the N_2 atmosphere for 150 days[21]. ALD is also a potential technology for fabricating the flexible, compatible, and scalable films. On different substrates (polymers, metals, metal sulfides, and oxides), PbI_2 films were first prepared through ALD processes with the deposition temperatures below 90 °C using $Pb(btsa)_2$ and SnI_4 as precursors. Moreover, ALD Al_2O_3 was used as an encapsulation layer which effectively protected the underlying PbI_2 film[78].

High-performance flexible PSCs need transparent electrodes with low fabrication temperature and reduced charge recombination losses. ALD layers could meet these requirements. Jin *et al.* have proposed a flexible electrode structure, silver nanowires (AgNWs)/ZnO/ALD TiO_2 with excellent transparency and electrical and mechanical characteristics[28]. The ALD TiO_2 layer was applied to effectively passivate the charge recombination defects on the ZnO layer and protect the perovskite layer from decomposition. The power conversion efficiency (PCE) of this flexible PSC reaches 17.11%, comparable to that of 18.26% of rigid devices. Finally, it maintained 77% of initial PCE after 2,000 bending cycles with a radius of 6 mm[28]. Because of the inferior gas barrier properties of plastic substrates, flexible devices often suffer from intrinsic problems of poor stability under ambient environments. Lin *et al.* investigated the stability of flexible PSCs under illumination for polyisobutylene (PIB)-, 1H,1H,2H,2H-perfluorooctyltriethoxysilane (PFOTES)/ZnO-, and ALD Al_2O_3-based polyethylene naphthalate/indium tin oxide (PEN/ITO) substrates[79]. Due to the compact and uniform ALD films, ALD Al_2O_3-based devices showed the best T_{80} (Normalized PCE of 0.8) value (increased from 80 h to over 350 h) under maximum power point (MPP) tracking under 1 sun illumination in ambient conditions [60%-70% relative humidity (RH)][79].

ALD layers always act as diffusion barriers, buffer layers, and recombination layers in tandem solar cells. Traditionally, all-perovskite tandem solar cells require several spin-coating steps, which limited the device area. For large areas, ALD is a scalable preparation technique to fabricate large area functional layers due to its good expandability. To overcome the problem of reaction between interfacial halide and metal electrode, Xiao *et al.* introduced a thin conformal diffusion barrier (CDB) consisting of 10 nm ALD SnO_2 to an all-perovskite tandem module[80]. The CDB layer could extract vertical electrons and serve as the lateral diffusion barrier between interconnecting subcells. The ITO/ALD SnO_2/Ag junction showed good ohmic contact, demonstrating that the CDB layer supported effective electrical interconnection between two subcells. Finally, they achieved a certified PCE of 21.7% with aperture area of 20.25 cm^2, and the modules with CDB maintained 75% of their initial efficiency for 500 h upon MPP tracking under 1 sun illumination in ambient conditions while the modules without CDB decreased to less than 50% after 20 h[80]. Yu *et al.*

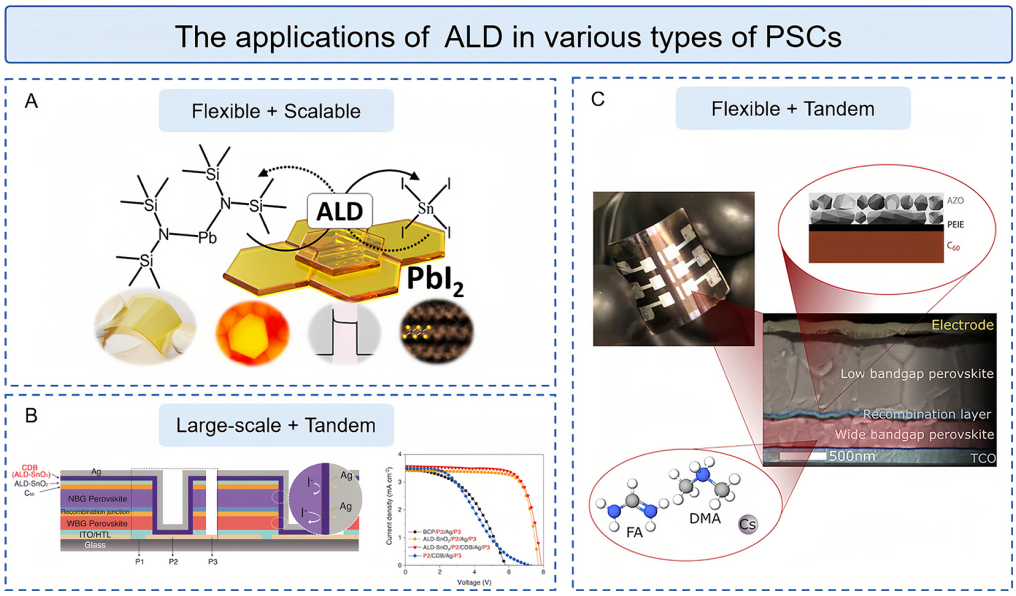

Figure 6. A scheme of the applications of ALD in different types of PSCs. (A) Perovskite material and encapsulation layer on flexible and scalable substrates. Reprinted with permission from ref.[78]. Copyright 2016 American Chemical Society. (B) Charge extractor and diffusion barrier in all-perovskite tandem solar modules. Reprinted with permission from ref.[80]. Copyright 2022 The American Association for the Advancement of Science. (C) Recombination layer in flexible all-perovskite tandem solar cells. Reprinted with permission from ref.[60]. Copyright 2019 Elsevier.

have developed a new strategy to activate the unreactive PCBM substrate and deposit an impermeable ALD sputtering buffer SnO_x layer[22]. For allowing the near-infrared light to pass through and be absorbed in the bottom subcell, tandem solar cells need the top subcell to be optical transmission; the dense ALD films are vital for the perovskite/silicon tandem solar cells when preparing transparent conductive oxides (TCOs) and avoid damage to the perovskite during sputtering. For demonstration, optimized ALD layers were employed as sputtering buffer layers in semi-transparent (ST) devices. As a result, the ratio of working devices to both working and non-working devices of optimized ST devices was almost 100%, exhibiting the excellent anti-sputtering ability[22]. As for all-perovskite tandem solar cells, the ideal recombination layer could enable voltage addition and optical loss reduction between the subcells. Palmstrom *et al.* introduced a modified structure with a ALD layer (C_{60}/PEIE/ALD AZO) to enhance the composite between low bandgap and wide bandgap perovskite layers, reducing solvent degradation of the active layer during solution deposition[60]. Recently, ALD SnO_x layers provided a promising solution to enhance carrier-selective contacts in tandem PSCs. Xiong *et al.* controlled the O:Sn ratio by varying the purge time of the oxygen source[81]. They found that the perovskite degraded apparently when the ratio increased, and the electrical properties became worse when the ratio decreased. By modifying the gradient compositions of the ALD SnO_x layer, the charge extraction ability was enhanced. Finally, they achieved a PCE of 28.9% and retained 95% of its initial efficiency for 500 h upon MPP tracking under AM 1.5G illumination for a 1.0 cm^2 monolithic perovskite/silicon tandem solar cell[81].

Stability issues in moisture, oxygen, and light exposure are key challenges for PSCs. As shown in Table 4, ALD could act as encapsulation barriers against external environmental factors, thereby improving the long-term stability of PSCs. As for p-i-n structure PSCs, Brinkmann *et al.* prepared 20 nm ALD SnO_x with water vapor transmittance as low as 7×10^{-5} g m^2 d^{-1}, showing the excellent water vapor barrier properties[55]. The ALD SnO_x layer could prevent decomposition products from being expelled from perovskite. Under inert atmosphere, the unencapsulated perovskite underwent thermal decomposition, as observed by

Table 4. Recent studies on improving the stability of perovskite devices by ALD

Buffer layer	Architecture	Efficiency	Storage condition	Stability of devices	Ref.
BCP	ITO/NiO_x/PTAA/Al_2O_3 /FAMACs/PCBM/BCP/Ag	N/A	Under UV light (365 nm) in air for 20 days; N_2 atmosphere (at 65 °C) for 1,080 h; Ambient air (at 25 °C, 60%RH) for 1,440 h; Heated at 85 °C with 85%RH in N_2 atmosphere for 110 h	A strong diffraction peak of PbI_2 was detected, and the color of the film faded from dark brown to yellow; Normalized PCE decreased to 0.70; Normalized PCE decreased to 0.73; Normalized PCE decreased to 0.22	[82]
ALD SnO_x	ITO/NiO_x/PTAA/Al_2O_3 /FAMACs/PCBM/ALD SnO_x/Ag	21.10%	Under UV light (365 nm) in air for 40 days; N_2 atmosphere (at 65 °C) for 1,080 h; Ambient air (at 25 °C, 60%RH) for 1,440 h; Heated at 85 °C with 85%RH in N_2 atmosphere for 680 h	A strong diffraction peak of PbI_2 was detected, and the color of the film faded from dark brown to yellow; Normalized PCE decreased to 0.82; Normalized PCE decreased to 0.85; Normalized PCE decreased to 0.38	
Modified-ALD SnO_x	ITO/NiO_x/PTAA/Al_2O_3 /FAMACs/PCBM:EVA/ ALD SnO_x/Ag	22.06%	Under UV light (365 nm) in air for 40 days; N_2 atmosphere (at 65 °C) for 1,080 h; Ambient air (at 25 °C, 60%RH) for 1,440 h; Heated at 85 °C with 85%RH in N_2 atmosphere for 800 h	A slight diffraction peak of PbI_2 was detected, and the color of the film showed no big change; Normalized PCE decreased to 0.90; Normalized PCE decreased to 0.92; Normalized PCE decreased to 0.85	
BCP	FTO/NiO_x/Me-4PACz/perovskite/C_{60} /BCP/Cu	24.29%	N_2 atmosphere (85%RH) for 10 h; MPP tracking at 85 °C in ambient air for 15 h; 85%RH at 85 °C for 150 h; Operated under 1 sun illumination in ambient air (30%~50%RH at 65 °C) for 67 h	Normalized PCE decreased to 0.65; Normalized PCE decreased to 0.61; Normalized PCE decreased to 0.78; Normalized PCE decreased to 0.90	[83]
ALD SnO_x	FTO/NiO_x/Me-4PACz/perovskite/C_{60} /ALD SnO_x/Cu	24.42%	N_2 atmosphere (85%RH) for 10 h; MPP tracking at 85 °C in ambient air for 15 h; 85%RH at 85 °C for 150 h; Operated under 1 sun illumination in ambient air (30%~50%RH at 65 °C) for 140 h	Normalized PCE decreased to 0.45; Normalized PCE decreased to 0.85; Normalized PCE decreased to 0.80; Normalized PCE decreased to 0.90;	
ALD AlO_x	FTO/NiO_x/Me-4PACz/perovskite/C_{60} /ALD AlO_x /Cu	24.61%	N_2 atmosphere (85%RH) for 10 h; MPP tracking at 85 °C in ambient air for 15 h; 85%RH at 85 °C for 150 h; Operated under 1 sun illumination in ambient air (30%~50%RH at 65 °C) for 1,150 h	Normalized PCE decreased to 0.80; Normalized PCE decreased to 0.97; Normalized PCE decreased to 0.90; Normalized PCE decreased to 0.90	
Spiro-OMeTAD	FTO/ ALD SnO_2/perovskite/Spiro-OMeTAD/ALD V_2O_{5-x}/Au	23.15%	Ambient air (at 24 °C, 20%RH) for 576 h; Operated under continuous AM 1.5G light illumination and a constant bias of 0.85 V without a UV cutoff filter for 130 h	Normalized PCE decreased to 0.318; Normalized PCE decreased to 0.712	[84]
ALD V_2O_{5-x}	FTO/ ALD SnO_2/perovskite/Spiro-OMeTAD/ALD V_2O_{5-x}/Au	23.02%	Ambient air (at 24 °C, 20%RH) for 576 h; Operated under continuous AM 1.5G light illumination and a constant bias of 0.85 V without a UV cutoff filter for 130 h	Normalized PCE decreased to 0.905; Normalized PCE decreased to 0.949	
Spiro-OMeTAD	F:SnO_2/SnO_2/perovskite/Spiro-OMeTAD/Au	19.1%	Ambient air for 300 days	Normalized PCE decreased to 0.38	[85]
ALD Al_2O_3	F:SnO_2/SnO_2/perovskite/Spiro-OMeTAD/ALD Al_2O_3/Au	19.4%	Ambient conditions for 300 days	Normalized PCE decreased to 0.84	
Spiro-OMeTAD	FTO/ALD SnO_2/SnO_2 NPs/perovskite/Spiro-OMeTAD/Au	21.29%	Operated under continuous AM 1.5G light illumination and a constant bias of 0.85 V without a UV cutoff filter for 120 h	Normalized PCE decreased to 0.832	[86]
ALD TiO_2	FTO/ALD SnO_2/SnO_2 NPs/perovskite/Spiro-OMeTAD/ALD TiO_2/Au	20.68%	Operated under continuous AM 1.5G light illumination and a constant bias of 0.85 V without a UV cutoff filter for 120 h	Normalized PCE decreased to 0.965	

characteristic peaks of PbI_2 [Figure 7A and B]. However, the ALD SnO_x-based device effectively hindered the outer diffusion of the decomposition products, significantly improving the thermal stability of the PSCs [Figure 7C][55]. Li *et al.* used the modified ALD SnO_x by ester groups of poly(ethylene-co-vinyl acetate) as a self-encapsulated interface, resulting in retaining 85% of the initial PCE after storage 85 °C with RH of 85% for over 800 h[82]. The choice of ALD materials is essential for the long-term stability level of PSCs. Recently, Zheng *et al.* systematically investigated the long-term stability and the underlying decomposition mechanisms of ALD SnO_x-based PSCs[83]. It was found that ALD SnO_x-based PSCs exhibited higher susceptibility to degradation, surpassing even the degradation levels observed with bathocuproine (BCP) under humid conditions. It further revealed that the ALD SnO_x layer triggered a phase transition in the perovskite when exposed to moisture, transitioning from the black cubic phase to the yellow δ phase despite the presence of a thin layer of fullerene between the SnO_x and the perovskite. Instead of SnO_x, ALD AlO_x layers emerged as a transformative strategy, sufficiently bolstering the humidity and thermal stability of the cells without affecting device efficiency. The optimized ALD AlO_x PSCs exhibited a PCE of 24.61% and maintained 88% of its initial efficiency after MPP tracking under 1 sun illumination for 1,350 h at 65°C in ambient air[83]. As for n-i-p PSCs, ALD V_2O_{5-x} deposited on the top of a Spiro-OMeTAD layer was utilized to block the moisture and oxygen, enhancing the stability by preserving the photovoltaic α-$FAPbI_3$ phase and eliminating the leakage of both Li ions from the intermediate layer and Au ions from the electrode [Figure 7D]. Finally, the PCE of ALD V_2O_{5-x}-based devices retained 90.5% of their initial efficiency after 576 h while that of the devices without ALD V_2O_{5-x} encapsulation layer reduced to 31.8% of the initial values in ambient condition (25%RH at 24 °C). In addition, the PCE of ALD V_2O_{5-x}-based devices maintained 94.9% of the initial efficiency after 130 h, while that of the devices without ALD V_2O_{5-x} encapsulation layers decreased to 71.2% of the initial PCE under operating conditions [Figure 7E and F]. The improved stability for PSCs with ALD V_2O_{5-x} was ascribed to the barrier function of ALD films and the retarded diffusion of Au electrodes by passivation of ALD layers[84].

CONCLUSION AND OUTLOOK

This paper reviews the influences of atomic layer precursors, deposition temperatures and reaction substrates on the physical and chemical properties of ALD films and the performance of PSCs. For the precursor, some metal sources may damage the substrate (such as perovskite, carrier transport layer, *etc.*). The physical properties (such as density, permeability, and resistivity) of the films prepared with different oxygen sources may change. Moreover, oxygen sources may also influence the device performance of PSCs, especially on FF. The deposition temperature also influences the characteristics of ALD films and the performance of ALD devices. The optimal deposition temperature can be obtained by testing the band gap, resistivity and absorptivity of the films prepared at different temperatures. The ALD substrate is also a crucial factor in the process of ALD. In the field of non-perovskite, there have been many studies on the substrate-inhibited island growth mode of ALD film. However, in perovskite, the reaction mechanism of ALD on different substrates is unclear, and most relevant studies are related to the stability of ALD perovskite devices prepared on various substrates and the water vapor barrier ability of ALD films.

At present, ALD is increasingly used in the carrier transport and encapsulation layers of PSCs. Therefore, this paper summarizes the influential factors (Especially for the reaction substrates) that need attention in preparing ALD films for PSCs, along with related solutions, which are conducive to the efficient and large-scale fabrication of PSCs and the related tandem cells.

Several challenges associated with ALD processing in perovskites need to be addressed:

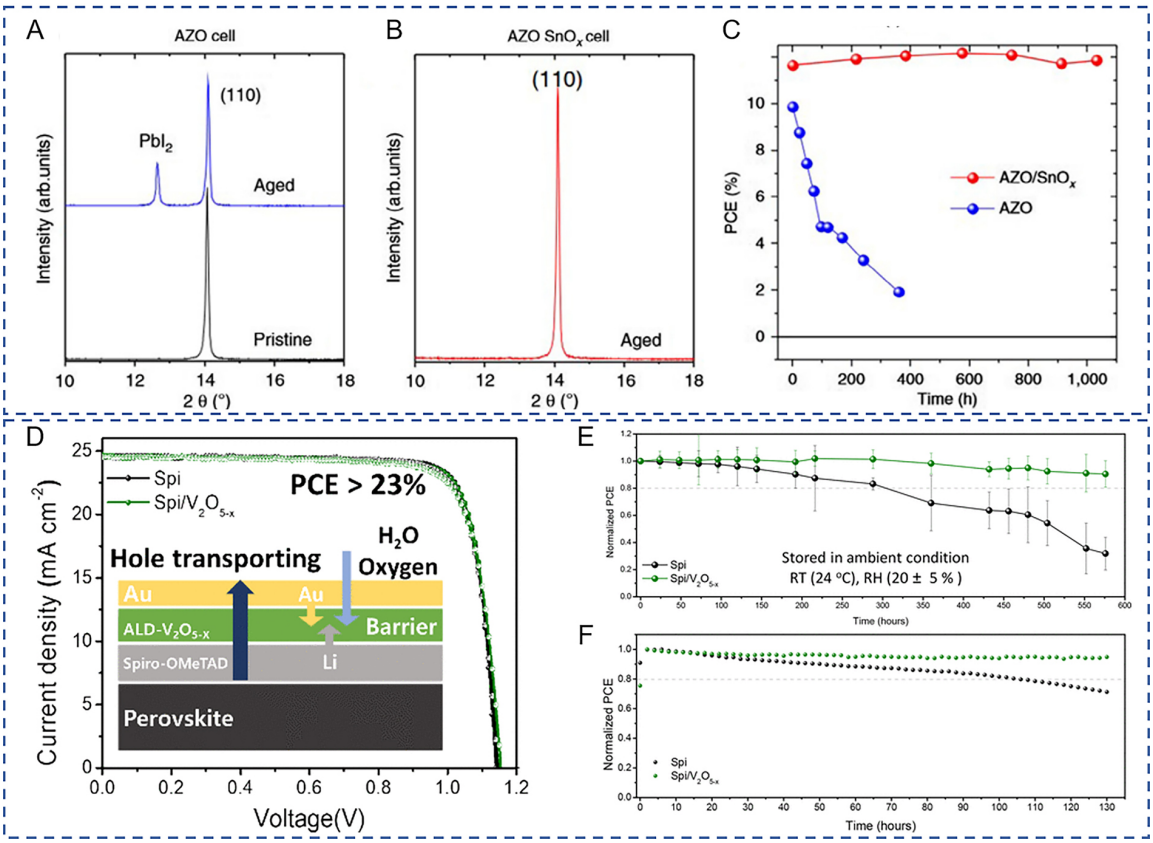

Figure 7. (A and B) XRD analysis of PSC with AZO and AZO/SnO_x before and after being heated in N_2 atmosphere for six days. (C) Thermal stability test (N_2 atmosphere at 60 °C). Reprinted with permission from ref.[55]. Copyright 2017 Nature Publishing Group. (D) Performance and structure of ALD V_2O_{5-x} based-PSC. (E) Ambient stability test (20%RH at 24 °C). (F) Operated stability test under AM 1.5G illumination. Reprinted with permission from ref.[84]. Copyright 2022 American Chemical Society.

Precursor selection and compatibility

Precursor selection is influenced by various factors, including chemical stability, vapor pressure, and reactivity. In the context of perovskite ALD, the choice of precursors must strike a delicate balance between providing the desired chemical composition and ensuring compatibility with the substrate material. For instance, while highly reactive precursors may offer enhanced film growth rates, they may also pose challenges in terms of substrate damage or film quality degradation due to uncontrolled reactions at the substrate surface. The compatibility between precursors and substrates encompasses several aspects, including adsorption kinetics, surface diffusion, and reaction kinetics. A precursor that exhibits favorable interactions with the substrate surface, such as strong adsorption and controlled surface diffusion, is more likely to result in uniform film growth. Conversely, mismatches in precursor-substrate compatibility can lead to non-uniform film coverage, defects, and reduced film quality. More experimental characterizations and computational models are needed to provide deeper insights into precursor-substrate interactions, guiding the optimization of ALD processes for diverse applications in PCSs.

Interfacial engineering

ALD enables the deposition of ultrathin, conformal layers with atomic-level precision, making it well-suited for interface engineering applications. It also offers opportunities for interface modification at the interface between the charge transport layers and electrodes. By depositing thin interfacial layers to promote adhesion, reduce interfacial resistance, and enhance charge collection efficiency, ALD can improve the

overall device performance and stability. Achieving precise control over interfacial properties, such as energy level alignment and interface roughness, is essential for maximizing device efficiency and stability.

Film uniformity

Achieving uniform deposition of functional layers using ALD across large-area substrates is crucial for scalability. Addressing issues such as precursor diffusion, surface coverage, and reaction kinetics to ensure uniform film deposition is essential.

Scalability and cost

Scaling up ALD processes for PSC production requires the development of high-throughput deposition methods compatible with large-area substrates. Addressing challenges related to deposition rate, precursor utilization, and equipment scalability is essential for transitioning ALD from laboratory-scale research to industrial-scale production. Cost-effective deposition techniques are necessary for the commercialization of PSCs. Optimizing ALD processes to minimize precursor consumption, reduce deposition time, and increase equipment efficiency can help lower production costs and make PSCs more competitive with traditional silicon-based photovoltaics.

DECLARATIONS

Authors' contributions

Proposed the topic of this mini review: Yu B, Yang Y
Performed literature survey: Yu B, Zhang J
Prepared the manuscript: Yu B, Zhang J
Collectively discussed and revised the manuscript: Yang Y, Yu D
Review, conceptualization, and supervision: Mai Y, Chen X

Availability of data and materials

Not applicable.

Financial support and sponsorship

This work was supported by Grant named the "One-Hundred Young Talents" of Guangdong University of Technology (No. 263113845).

Conflicts of interest

All authors declared that there are no conflicts of interest.

Ethical approval and consent to participate

Not applicable.

Consent for publication

Not applicable.

REFERENCES

1. Suntola T. Atomic layer epitaxy. *Mater Sci Rep* 1989;4:261-312. DOI
2. Santinacci L. Atomic layer deposition: an efficient tool for corrosion protection. *Curr Opin Colloid Interface Sci* 2023;63:101674. DOI
3. O'Neill BJ, Jackson DHK, Lee J, et al. Catalyst design with atomic layer deposition. *ACS Catal* 2015;5:1804-25. DOI

4. Bakke JR, Pickrahn KL, Brennan TP, Bent SF. Nanoengineering and interfacial engineering of photovoltaics by atomic layer deposition. *Nanoscale* 2011;3:3482-508. DOI PubMed
5. Hossain MA, Khoo KT, Cui X, et al. Atomic layer deposition enabling higher efficiency solar cells: a review. *Nano Mater Sci* 2020;2:204-26. DOI
6. Raiford JA, Oyakhire ST, Bent SF. Applications of atomic layer deposition and chemical vapor deposition for perovskite solar cells. *Energy Environ Sci* 2020;13:1997-2023. DOI
7. Xing Z, Xiao J, Hu T, et al. Atomic layer deposition of metal oxides in perovskite solar cells: present and future. *Small Methods* 2020;4:2000588. DOI
8. Sinha S, Nandi DK, Pawar PS, Kim SH, Heo J. A review on atomic layer deposited buffer layers for Cu(In,Ga)Se_2(CIGS) thin film solar cells: past, present, and future. *Solar Energy* 2020;209:515-37. DOI
9. Eperon GE, Stranks SD, Menelaou C, Johnston MB, Herz LM, Snaith HJ. Formamidinium lead trihalide: a broadly tunable perovskite for efficient planar heterojunction solar cells. *Energy Environ Sci* 2014;7:982-8. DOI
10. De Wolf S, Holovsky J, Moon SJ, et al. Organometallic halide perovskites: sharp optical absorption edge and its relation to photovoltaic performance. *J Phys Chem Lett* 2014;5:1035-9. DOI
11. Saliba M, Matsui T, Domanski K, et al. Incorporation of rubidium cations into perovskite solar cells improves photovoltaic performance. *Science* 2016;354:206-9. DOI
12. George SM. Atomic layer deposition: an overview. *Chem Rev* 2010;110:111-31. DOI PubMed
13. Yang Y, Luo Y, Ma S, Zhu C, Zhu L, Guo X. Advances of electron transport materials in perovskite solar cells: synthesis and application. *Prog Chem* 2021;33:281-302. DOI
14. Lobe S, Bauer A, Uhlenbruck S, Fattakhova-Rohlfing D. Physical vapor deposition in solid-state battery development: from materials to devices. *Adv Sci* 2021;8:e2002044. DOI PubMed PMC
15. Wang M, Carmalt CJ. Film fabrication of perovskites and their derivatives for photovoltaic applications via chemical vapor deposition. *ACS Appl Energy Mater* 2022;5:5434-48. DOI
16. Brinkmann KO, Gahlmann T, Riedl T. Atomic layer deposition of functional layers in planar perovskite solar cells. *Solar RRL* 2020;4:1900332. DOI
17. Gordon RG, Hausmann D, Kim E, Shepard J. A kinetic model for step coverage by atomic layer deposition in narrow holes or trenches. *Chem Vap Depos* 2003;9:73-8. DOI
18. Puurunen RL. Surface chemistry of atomic layer deposition: a case study for the trimethylaluminum/water process. *J Appl Phys* 2005;97:121301. DOI
19. Putkonen M, Niinistö L. Organometallic precursors for atomic layer deposition. In: Precursor chemistry of advanced materials, Fischer RA, editor. Berlin: Springer; 2005. pp. 125-45. DOI
20. Richey NE, de Paula C, Bent SF. Understanding chemical and physical mechanisms in atomic layer deposition. *J Chem Phys* 2020;152:040902. DOI
21. Zhao R, Zhang K, Zhu J, et al. Surface passivation of organometal halide perovskites by atomic layer deposition: an investigation of the mechanism of efficient inverted planar solar cells. *Nanoscale Adv* 2021;3:2305-15. DOI PubMed PMC
22. Yu B, Tang F, Yang Y, et al. Impermeable atomic layer deposition for sputtering buffer layer in efficient semi-transparent and tandem solar cells via activating unreactive substrate. *Adv Mater* 2023;35:e2202447. DOI
23. Zhang Y, Yang Y, Mbumba MT, et al. Research progress of buffer layer and encapsulation layer prepared by atomic layer deposition to improve the stability of perovskite solar cells. *Solar RRL* 2022;6:2200823. DOI
24. Lee KM, Chang SH, Wang KH, et al. Thickness effects of ZnO thin film on the performance of tri-iodide perovskite absorber based photovoltaics. *Solar Energy* 2015;120:117-22. DOI
25. Matsui T, Bivour M, Hermle M, Sai H. Atomic-layer-deposited TiO_x nanolayers function as efficient hole-selective passivating contacts in silicon solar cells. *ACS Appl Mater Interfaces* 2020;12:49777-85. DOI PubMed
26. Correa Baena JP, Steier L, Tress W, et al. Highly efficient planar perovskite solar cells through band alignment engineering. *Energy Environ Sci* 2015;8:2928-34. DOI
27. Zardetto V, di Giacomo F, Lifka H, et al. Surface fluorination of ALD TiO_2 electron transport layer for efficient planar perovskite solar cells. *Adv Mater Inter* 2018;5:1701456. DOI
28. Jin TY, Li W, Li YQ, et al. High-performance flexible perovskite solar cells enabled by low-temperature ALD-assisted surface passivation. *Adv Opt Mater* 2018;6:1801153. DOI
29. Choudhury D, Rajaraman G, Sarkar SK. Self limiting atomic layer deposition of Al_2O_3 on perovskite surfaces: a reality? *Nanoscale* 2016;8:7459-65. DOI PubMed
30. Kuang Y, Zardetto V, van Gils R, et al. Low-temperature plasma-assisted atomic-layer-deposited SnO_2 as an electron transport layer in planar perovskite solar cells. *ACS Appl Mater Interfaces* 2018;10:30367-78. DOI PubMed PMC
31. Lee Y, Lee S, Seo G, et al. Efficient planar perovskite solar cells using passivated tin oxide as an electron transport layer. *Adv Sci* 2018;5:1800130. DOI PubMed PMC
32. Hu T, Becker T, Pourdavoud N, et al. Indium-free perovskite solar cells enabled by impermeable tin-oxide electron extraction layers. *Adv Mater* 2017;29:1606656. DOI
33. Ren N, Zhu C, Li R, et al. 50 °C low-temperature ALD SnO_2 driven by H_2O_2 for efficient perovskite and perovskite/silicon tandem solar cells. *Appl Phys Lett* 2022;121:033502. DOI

34. Hultqvist A, Aitola K, Sveinbjörnsson K, et al. Atomic layer deposition of electron selective SnO_x and ZnO films on mixed halide perovskite: compatibility and performance. *ACS Appl Mater Interfaces* 2017;9:29707-16. DOI
35. Zardetto V, Williams BL, Perrotta A, et al. Atomic layer deposition for perovskite solar cells: research status, opportunities and challenges. *Sustain Energy Fuels* 2017;1:30-55. DOI
36. Kruszyńska J, Ostapko J, Ozkaya V, et al. Atomic layer engineering of aluminum-doped zinc oxide films for efficient and stable perovskite solar cells. *Adv Mater Inter* 2022;9:2200575. DOI
37. Behrendt A, Friedenberger C, Gahlmann T, et al. Highly robust transparent and conductive gas diffusion barriers based on tin oxide. *Adv Mater* 2015;27:5961-7. DOI
38. Wang H, Liu Y, Liu H, et al. Effect of various oxidants on reaction mechanisms, self-limiting natures and structural characteristics of Al_2O_3 films grown by atomic layer deposition. *Adv Mater Inter* 2018;5:1701248. DOI
39. Lee SU, Park H, Shin H, Park NG. Atomic layer deposition of SnO_2 using hydrogen peroxide improves the efficiency and stability of perovskite solar cells. *Nanoscale* 2023;15:5044-52. DOI
40. Kim H. Characteristics and applications of plasma enhanced-atomic layer deposition. *Thin Solid Films* 2011;519:6639-44. DOI
41. Kim H. Atomic layer deposition of metal and nitride thin films: current research efforts and applications for semiconductor device processing. *J Vac Sci Technol B* 2003;21:2231-61. DOI
42. Johnson RW, Hultqvist A, Bent SF. A brief review of atomic layer deposition: from fundamentals to applications. *Mater Today* 2014;17:236-46. DOI
43. Potts SE, Keuning W, Langereis E, Dingemans G, van de Sanden MCM, Kessels WMM. Low temperature plasma-enhanced atomic layer deposition of metal oxide thin films. *J Electrochem Soc* 2010;157:P66. DOI
44. Muñoz-Rojas D, Macmanus-Driscoll J. Spatial atmospheric atomic layer deposition: a new laboratory and industrial tool for low-cost photovoltaics. *Mater Horiz* 2014;1:314-20. DOI
45. Poodt P, Knaapen R, Illiberi A, Roozeboom F, van Asten A. Low temperature and roll-to-roll spatial atomic layer deposition for flexible electronics. *J Vac Sci Technol A* 2012;30:01A142. DOI
46. Illiberi A, Roozeboom F, Poodt P. Spatial atomic layer deposition of zinc oxide thin films. *ACS Appl Mater Interfaces* 2012;4:268-72. DOI PubMed
47. Lindahl J, Hägglund C, Wätjen JT, Edoff M, Törndahl T. The effect of substrate temperature on atomic layer deposited zinc tin oxide. *Thin Solid Films* 2015;586:82-7. DOI
48. Chistiakova G, Mews M, Wilks RG, Bär M, Korte L. In-system photoelectron spectroscopy study of tin oxide layers produced from tetrakis(dimethylamino)tin by plasma enhanced atomic layer deposition. *J Vac Sci Technol A* 2018;36:02D401. DOI
49. Köhnen E, Jošt M, Morales-Vilches AB, et al. Highly efficient monolithic perovskite silicon tandem solar cells: analyzing the influence of current mismatch on device performance. *Sustain Energy Fuels* 2019;3:1995-2005. DOI
50. Hultqvist A, Jacobsson TJ, Svanström S, et al. SnO_x atomic layer deposition on bare perovskite-an investigation of initial growth dynamics, interface chemistry, and solar cell performance. *ACS Appl Energy Mater* 2021;4:510-22. DOI PubMed PMC
51. Schulze TF, Korte L, Ruske F, Rech B. Band lineup in amorphous/crystalline silicon heterojunctions and the impact of hydrogen microstructure and topological disorder. *Phys Rev B* 2011;83:165314. DOI
52. Puurunen RL, Vandervorst W. Island growth as a growth mode in atomic layer deposition: a phenomenological model. *J Appl Phys* 2004;96:7686-95. DOI
53. Labbe M, Cadien K, Ivey DG. Growth of multiple island layers during iron oxide atomic layer deposition: an electron microscopy and spectroscopic ellipsometry investigation. *J Phys Chem C* 2022;126:19883-94. DOI
54. Gilmer GH, Grabow MH. Models of thin film growth modes. *JOM* 1987;39:19-23. DOI
55. Brinkmann KO, Zhao J, Pourdavoud N, et al. Suppressed decomposition of organometal halide perovskites by impermeable electron-extraction layers in inverted solar cells. *Nat Commun* 2017;8:13938. DOI PubMed PMC
56. Yu X, Yan H, Peng Q. Improve the stability of hybrid halide perovskite via atomic layer deposition on activated phenyl-C_{61} butyric acid methyl ester. *ACS Appl Mater Interfaces* 2018;10:28948-54. DOI
57. Gong J, Adnani M, Jones BT, et al. Nanoscale encapsulation of hybrid perovskites using hybrid atomic layer deposition. *J Phys Chem Lett* 2022;13:4082-9. DOI
58. Wang W, Yang Z, Ding J, Kong J, Li X. Improving water-resistance of inverted flexible perovskite solar cells via tailoring the top electron-selective layers. *Solar Energy Mater Solar Cells* 2022;238:111609. DOI
59. Liu J, Wu Y, Zhao Z, et al. Reducing damage of sputtering and improving conductivity of transparent electrodes for efficient semi-transparent perovskite solar cells. *J Phys D Appl Phys* 2023;56:365101. DOI
60. Palmstrom AF, Eperon GE, Leijtens T, et al. Enabling flexible all-perovskite tandem solar cells. *Joule* 2019;3:2193-204. DOI
61. Li W, Xu YX, Wang D, Chen F, Chen ZK. Inorganic perovskite light emitting diodes with ZnO as the electron transport layer by direct atomic layer deposition. *Org Electron* 2018;57:60-7. DOI
62. Raiford JA, Boyd CC, Palmstrom AF, et al. Enhanced nucleation of atomic layer deposited contacts improves operational stability of perovskite solar cells in air. *Adv Energy Mater* 2019;9:1902353. DOI
63. Yun HJ, Kim H, Choi BJ. Nucleation and growth behavior of aluminum nitride film using thermal atomic layer deposition. *Ceram Int* 2020;46:13372-6. DOI
64. Baji Z, Lábadi Z, Horváth ZE, et al. Nucleation and growth modes of ALD ZnO. *Cryst Growth Des* 2012;12:5615-20. DOI
65. Uğur A, Savacı U, Ay N, Turan S. Growth of ultrathin Al_2O_3 islands on hBN particles by atomic layer deposition in a custom fluidized

bed reactor using $Al(CH_3)_3$ and H_2O. *Appl Surf Sci* 2021;537:147665. DOI

66. Hagen DJ, Connolly J, Povey IM, Rushworth S, Pemble ME. Island coalescence during film growth: an underestimated limitation of Cu ALD. *Adv Mater Inter* 2017;4:1700274. DOI
67. Wilson CA, Grubbs RK, George SM. Nucleation and growth during Al_2O_3 atomic layer deposition on polymers. *Chem Mater* 2005;17:5625-34. DOI
68. Jur JS, Spagnola JC, Lee K, Gong B, Peng Q, Parsons GN. Temperature-dependent subsurface growth during atomic layer deposition on polypropylene and cellulose fibers. *Langmuir* 2010;26:8239-44. DOI PubMed
69. Demelius L, Blatnik M, Unger K, Parlanti P, Gemmi M, Coclite AM. Shedding light on the initial growth of ZnO during plasma-enhanced atomic layer deposition on vapor-deposited polymer thin films. *Appl Surf Sci* 2022;604:154619. DOI
70. Weiß A, Goldmann J, Kettunen S, et al. Conversion of ALD CuO thin films into transparent conductive p-type CuI thin films. *Adv Mater Inter* 2023;10:2201860. DOI
71. Zhou J, Huang Q, Zhao Q, et al. Performance promotion of aluminum oxide capping layer through interface engineering for tunnel oxide passivating contacts. *Solar Energy Mater Solar Cells* 2022;245:111865. DOI
72. Hagedorn S, Knauer A, Weyers M, Naumann F, Gargouri H. AlN and AlN/Al_2O_3 seed layers from atomic layer deposition for epitaxial growth of AlN on sapphire. *J Vac Sci Technol A* 2019;37:020914. DOI
73. Lin G, Zhao MQ, Jia M, et al. Performance enhancement of monolayer MoS_2 transistors by atomic layer deposition of high- *k* dielectric assisted by Al_2O_3 seed layer. *J Phys D Appl Phys* 2020;53:105103. DOI
74. Yang H, Xiang D, Mao H, et al. Native oxide seeded spontaneous integration of dielectrics on exfoliated black phosphorus. *ACS Appl Mater Interfaces* 2020;12:24411-8. DOI
75. Wolff CM, Caprioglio P, Stolterfoht M, Neher D. Nonradiative recombination in perovskite solar cells: the role of interfaces. *Adv Mater* 2019;31:e1902762. DOI PubMed
76. Xia J, Sohail M, Nazeeruddin MK. Efficient and stable perovskite solar cells by tailoring of interfaces. *Adv Mater* 2023;35:e2211324. DOI PubMed
77. Zhao W, Duan Y. Advanced applications of atomic layer deposition in perovskite-based solar cells. *Adv Photonics Res* 2021;2:2100011. DOI
78. Popov G, Mattinen M, Hatanpää T, et al. Atomic layer deposition of PbI_2 thin films. *Chem Mater* 2019;31:1101-9. DOI
79. Lin J, He Y, Mo H, et al. Substrate modifications for stability improvements of flexible perovskite solar cells. *Energy Technol* 2024;12:2300958. DOI
80. Xiao K, Lin YH, Zhang M, et al. Scalable processing for realizing 21.7%-efficient all-perovskite tandem solar modules. *Science* 2022;376:762-7. DOI
81. Xiong Z, Wu L, Zhou X, et al. Constructing tin oxides interfacial layer with gradient compositions for efficient perovskite/silicon tandem solar cells with efficiency exceeding 28%. *Small* 2024;20:e2308024. DOI
82. Li J, Xing Z, Li D, et al. Suppressed ion migration in FA-rich perovskite photovoltaics through enhanced nucleation of encapsulation interface. *Small* 2024;20:e2305732. DOI
83. Zheng Z, Xue Z, Zhao K, et al. Unveiling and overcoming instabilities in perovskite solar cells induced by atomic-layer-deposition tin oxide. *Solar RRL* 2024;8:2301076. DOI
84. Park H, Jeong S, Kim E, Shin S, Shin H. Hole-transporting vanadium-containing oxide (V_2O_{5-x}) interlayers enhance stability of α-$FAPbI_3$-based perovskite solar cells (~23%). *ACS Appl Mater Interfaces* 2022;14:42007-17. DOI
85. Singh R, Ghosh S, Subbiah AS, Mahuli N, Sarkar SK. ALD Al_2O_3 on hybrid perovskite solar cells: unveiling the growth mechanism and long-term stability. *Solar Energy Mater Solar Cells* 2020;205:110289. DOI
86. Seo S, Shin S, Kim E, Jeong S, Park NG, Shin H. Amorphous TiO_2 coatings stabilize perovskite solar cells. *ACS Energy Lett* 2021;6:3332-41. DOI